Journal of Biomechanics 177 (2024) 112379

Contents lists available at ScienceDirect

Journal of Biomechanics

journal homepage: www.elsevier.com/locate/jbiomech

The influence of load carriage and prosthetic foot type on individual muscle and prosthetic foot contributions to body support and propulsion

Aude S. Lefranc [a], Glenn K. Klute [b,c], Richard R. Neptune [a,*]

[a] Walker Department of Mechanical Engineering, The University of Texas at Austin, Austin, TX, USA
[b] Department of Veteran Affairs, Center for Limb Loss and MoBility, Seattle, WA, USA
[c] Department of Mechanical Engineering, University of Washington, Seattle, WA, USA

ARTICLE INFO

Keywords:
Lower limb amputation
Load carriage
Gait, biomechanics
Muscle function
Modeling and simulation

ABSTRACT

Individuals with transtibial amputation (TTA) experience altered gait mechanics, which are primarily attributed to the functional loss of the ankle plantarflexors. The plantarflexors contribute to body support and propulsion and play an important role in adapting to different load carriage conditions. However, how muscle function is altered across different prosthetic foot types and load carriage scenarios for individuals with TTA remains unclear. This study used musculoskeletal modeling and simulation of human movement in OpenSim to investigate the effects of a range of prosthetic feet and load conditions on individual muscle and prosthetic foot contributions to body support and propulsion. Twenty walking trials were collected from five individuals with TTA, consisting of five loading conditions (no-load; 30 lbs (13.6 kg) carried as a front-load, back-load, intact-side-load and residual-side-load) while wearing four prosthetic feet (their passive standard of care (SOC) foot, their SOC foot one category stiffer, their SOC foot with a heel stiffening wedge, and a dual-keel foot). Two participants also wore a powered ankle–foot prosthesis, thus completing an additional five trials each. The results indicated that the front-load condition may be more challenging because it required overall increased muscle contributions to body support and propulsion. However, the front- and residual-side-loads required reduced intact-side plantarflexor contributions to support and propulsion, and thus may be advantageous for individuals with plantarflexor weakness. Further, the large variability across contributions suggests that individuals with TTA may rely on a variety of compensatory mechanisms depending on the load condition and prosthetic foot used.

1. Introduction

Individuals with unilateral transtibial amputation (TTA) display reduced walking speeds, increased bilateral asymmetry and increased incidence of intact-leg osteoarthritis compared to non-amputees (Burke et al., 1978; Robinson et al., 1977; Sanderson & Martin, 1997). These deficits are partially attributed to the functional loss of the ankle plantarflexors, which are essential to providing body support and propulsion, leg-swing initiation and balance control (Liu et al., 2006; Neptune et al., 2001, 2004; Neptune & McGowan, 2011, 2016; Pandy et al., 2010; Zajac et al., 2003). Most clinically prescribed prosthetic foot–ankle devices are passive and cannot provide the biomechanical function of active ankle muscles, resulting in a need for compensations from other lower-limb muscles.

Load carriage adds another layer of complexity to the biomechanics of amputee walking. Many activities of daily living require various forms of load carriage including carrying infants or toddlers (often side-loads), pregnancy or picking up boxes (front-loads) or walking to class with a backpack (back-load). Front-, back- and side-loads notably affect postural and spatiotemporal gait parameters in unimpaired populations (Simpkins et al., 2022; Singh and Koh, 2009; Crosbie et al., 1994). Back-loads, which are the most extensively investigated load carriage position, have been shown to result in increased trunk, hip and knee flexion, increased hip and knee extension moments and increased muscle activation of lower limb and trunk muscles (Walsh and Low, 2021). For non-amputees, the plantarflexors play a critical role in adapting to load carriage, with the mechanical power generated by the ankle being modulated to accommodate additional demand (McGowan et al., 2008, 2009). Musculoskeletal modeling and simulation have been used to analyze individual muscle and prosthetic foot–ankle contributions to

* Corresponding author at: Walker Department of Mechanical Engineering, The University of Texas at Austin, 204 E. Dean Keeton Street, Stop C2200, Austin, TX 78712-1591, USA.
E-mail address: rneptune@mail.utexas.edu (R.R. Neptune).

https://doi.org/10.1016/j.jbiomech.2024.112379
Accepted 18 October 2024
Available online 20 October 2024

body support and propulsion and highlighted the importance of the plantarflexor muscles in maintaining natural gait during unloaded amputee walking (Silverman & Neptune, 2012; Zmitrewicz et al., 2007). However, individuals with TTA cannot modulate ankle power on the residual-side to adapt to accommodate load changes.

Prosthetic feet are not available in a continuous range of stiffnesses but are instead manufactured in discrete ordinal categories, which are prescribed based on an individual's anticipated activity level and body weight, where most widely prescribed models have a relatively narrow weight range of 10 kg for each category. Thus, when amputees carry a load, the added weight often exceeds the range of the prescribed stiffness category. As a result, individuals carrying a load with passive feet exhibit greater increases in metabolic cost relative to unimpaired individuals, as well as increased intact limb power generation and absorption and increased residual foot dorsiflexion during late stance (Doyle et al., 2014, 2015; Schnall et al., 2012, 2014).

While previous work suggests that using a powered-ankle prosthesis results in decreased metabolic cost, increased trailing residual-leg mechanical work and other gait benefits (e.g., Herr & Grabowski, 2012; Montgomery & Grabowski, 2018), it is unclear whether those benefits remain during load carriage. Further, few studies have compared commonly used prosthetic foot designs such as standard-of-care (SOC) feet with different stiffness categories, SOC feet with a stiffening heel wedge, and dual-keel feet during loaded walking.

The purpose of this study was to use musculoskeletal modeling and simulation to investigate the effects of several prosthetic feet and load conditions on individual muscle and prosthesis contributions to body support and propulsion. We expected that during load carriage, stiffer prosthetic feet would result in increased prosthetic foot contributions to body support and propulsion relative to the SOC foot, while reducing muscle contributions. Further, we expected that a powered foot would result in the largest foot contributions to body support and propulsion for all load conditions. Finally, we expected that there would be an optimal load carriage position which maximized prosthetic foot contributions while minimizing muscle contributions to support and propulsion.

2. Methods

2.1. Musculoskeletal model

A generic musculoskeletal model with 23 degrees of freedom and 92 musculotendon actuators (Delp et al., 2007; Seth et al., 2018) was modified to create a three-dimensional TTA model by removing the segments distal to the residual knee and replacing them with a transected tibia, pylon-socket and ankle–foot prosthesis with inertial properties adapted from LaPrè et al. (2018). The knee and intact ankle joints were modeled as one degree of freedom pin joints (Fey et al., 2012; Silverman & Neptune, 2012), while the hip joint was modeled with three degrees of freedom. The six degrees of freedom between the transected tibia and pylon-socket segment were locked and all muscles crossing the ankle joint were removed. To simulate the effect of a prosthetic ankle rather than provide a realistic representation of the prosthetic ankle itself, we used a coordinate actuator at the ankle joint to apply a proportional torque to achieve the desired experimentally measured ankle kinematics. To verify that the coordinate actuator effectively simulated the prosthetic ankle, the computed muscle control (CMC) obtained ankle torques were compared with ankle torques derived from inverse dynamics (root-mean square error = 4.307 N*m, error standard deviation across trials = 1.113 N*m). To model the various loading conditions, a 30 lbs (13.6 kg) pack was attached to the front, back, intact and residual-side of the torso segment with inertial properties adapted from Dembia et al. (2017). The interface between the mass and torso was modelled using a linear spring and damper, with their parameters adjusted for each trial so that the pack translation closely matched their experimentally measured values.

2.2. Data collection

Kinematic, kinetic and electromyography (EMG) data were collected from five individuals with TTA (Table 1) walking at their self-selected walking speed (SSWS). Kinematic and kinetic data were filtered with a fourth-order low-pass Butterworth filter with cutoff frequencies of 6 Hz and 15 Hz, respectively. EMG data were high-pass filtered at 40 Hz, demeaned, rectified, low-pass filtered at 4 Hz, and normalized to the peak activation per trial. All participants provided informed consent before participating in this Institutional Review Board (IRB) approved protocol. Sixty-two reflective markers were placed on each participant using a modified Vicon's Plug-in-Gait full-body model, which included additional markers located on the medial malleolus, medial elbow, and first and fifth metatarsal heads. Marker clusters were used to track the thigh and upper arm segments and the shank segments were tracked with markers placed on the fibular head and tibial tuberosity. Three markers were placed on the pack to track translation relative to the trunk. Kinematic data were collected using a 12-camera Vicon system (Vicon, Centennial, CO) and GRF data using five overground force plates (AMTI, Watertown, MA). Participants were instructed to walk in a straight line across the force plates at their SSWS. Only trials with a single, complete foot contact on the force plates were included in the analysis. Each participant was fit with the following five prostheses:

1. SOC foot of prescribed stiffness (PR)
2. SOC foot one-category stiffer (SF)
3. SOC foot with a heel-stiffening wedge (HW)
4. Dual-keel foot (DK)
5. Powered ankle–foot (PW)

The SOC foot, the one-category stiffer foot and the foot with a heel-stiffening wedge was the Sierra (Freedom Innovations). The SOC foot is a passive, clinically-prescribed, single-keeled foot, which can be used in conjunction with a heel wedge which reduces deflection of the keel. The dual-keel foot selected was the Thrive (Freedom Innovations), which is a passive foot that consists of a longer primary keel and a shorter secondary keel. Under no load conditions, only the primary keel is engaged. Under load carriage conditions, the heel keel deflects until it contacts a more proximal heel-stiffening bumper and then as the primary keel experiences greater deflections it engages the secondary keel. The powered ankle–foot was the Empower (Otto Bock). The loading conditions were as follows:

1. No-load
2. Front-load
3. Back-load
4. Intact-side-load
5. Residual-side-load

For the loaded conditions, subjects wore a weighted pack (30 lbs, 13.6 kg) fitted with additional straps securing it to their torso (Ergobaby). Subjects were given up to 15 min to walk with each condition to learn how each foot and load felt. The order of load carriage conditions and study feet worn were randomized for each subject.

2.3. Simulation analyses

For each subject and condition, a complete gait cycle was simulated using OpenSim 4.1 (Delp et al., 2007; Seth et al., 2018). Each simulation was validated to confirm that the kinematic errors, reserve actuators and residual forces were all within OpenSim's best practices range (Hicks et al., 2015), and that the simulation muscle activations closely aligned with the EMG data (Appendix A). The model was scaled so that it matched the kinematic data. Inverse kinematics was used to calculate joint angles. A residual-reduction algorithm was used to adjust model mass properties and movement to minimize dynamic inconsistencies

Table 1
Subject demographics.

Subject	Age (years)	Sex	Height (mm)	Mass (kg)	Side of Amputation	Time Since Amputation (Years)
1	40	Male	1799	101.5	Left	14
2	60	Male	1800	111.9	Right	3
3	39	Male	1712	105.7	Right	12
4	25	Female	1565	53.4	Right	24
5	43	Male	1820	107.0	Left	1
Mean ± standard deviation	41 +/- 12	–-	1739 ± 105	95.9 ± 24.0	–-	10 ± 9

between the measured ground reaction forces and body segment kinematics.

CMC was used to determine the muscle excitations needed for the model and experimental kinematics to match. CMC seeks to minimize experimental and simulation kinematic errors by using a combination of proportional-derivative control and static optimization (Thelen and Anderson, 2006). Subsequent analyses quantified the contributions of the prosthetic foot and each functional muscle group (Table 2) to body support (vertical GRF) and propulsion (anterior-posterior GRFs) (Hamner et al., 2010; Liu et al., 2006). Each contribution was integrated with respect to time over the stance phase and normalized by body weight. The contributions to propulsion were also normalized by walking speed.

3. Results

3.1. Effect of load carriage on muscle contributions to support

The intact-side muscles responded more to load changes than the corresponding muscles in the residual limb (e.g., GMAX, Figs. 1- 2). Further, the magnitude of the intact muscle contributions to support across all conditions was greater than that of the corresponding residual muscles (Figs. 1-2).

3.1.1. Changes relative to the prescribed foot condition

Wearing a non-prescribed foot typically resulted in an increased contribution to support from the prosthetic foot relative to the PR foot (Fig. 3). During load carriage, the PW foot resulted in reduced muscle contributions to support from both VAS (Fig. 3), relative to the PR foot. Wearing a non-prescribed foot generally resulted in a reduction in contribution to support from $VAS_{i,r}$, $GMAX_{i,r}$ and $GMED_i$ (Fig. 3) for the side-loads. $GMAX_r$ contributions to support increased while using the PW foot relative to the PR foot (Fig. 3). Further, all non-prescribed feet resulted in increased $GMAX_{i,r}$ contributions for the front-load condition, increased $GMED_r$ contributions for the residual-side-load condition, and decreased $GMED_i$ contributions for the residual-side-load condition contributions (Fig. 3).

3.1.2. Changes relative to the no-load condition

Carrying a load resulted in increased prosthetic foot contribution to support across all loading conditions and prosthetic feet (Fig. 4), where the intact-side-load resulted in the largest increase in prosthetic foot contribution. GAS responded to load similarly to the prosthetic foot (Fig. 4), which displayed the greatest increase in contribution to support during the intact-side- and back-load conditions relative to the no-load condition. Conversely, SOL responded inconsistently to the back-load condition (Fig. 4). However, the front- and intact-side-load conditions displayed the largest increase in contribution to support, relative to the no-load condition. $VAS_{i,r}$ had mixed responses to load carriage (Fig. 4), where the change in contribution to support varied depending on load condition or prosthesis worn. They displayed reduced contributions to support during the intact-side-load condition, as well as during PW foot use across most loaded conditions (Fig. 4). $GMAX_{i,r}$ displayed large increases in their contribution to support during loaded versus the no-load condition (Fig. 4) and was most apparent for the residual-side-load.

3.2. Muscle contributions to propulsion

The prosthetic foot contributed more to braking than the intact plantarflexors across all conditions (Figs. 5-6). GAS contributed most to forward propulsion for the back- and residual-side-load conditions (Fig. 6). However, SOL and the prosthetic foot contributed the most during the intact-side-load condition (Figs. 5-6). On average, $VAS_{i,r}$ contributed the most to braking for the front-load condition (Figs. 5-6). Both HAM also contributed the most to forward propulsion during the front-load, and the least during the back-load condition (Figs. 5-6).

3.2.1. Changes relative to the prescribed foot condition

The participants displayed reduced contributions to forward propulsion from their prosthesis for all loading conditions when wearing the PW relative to the PR foot (Fig. 7). Further, wearing a non-prescribed foot resulted in reduced prosthesis contributions to propulsion for the no-load and residual-side-load conditions (Fig. 7). Similarly, the intact plantarflexors reduced their contributions to propulsion when wearing a non-prescribed foot for the residual-side-load condition (Fig. 7), and the

Table 2
Functional groups analyzed. Shaded muscles were not included in the residual leg of the amputee model.

Group	Muscles/Actuators
FOOT	Prosthetic Foot
RF	Rectus Femoris
VAS	Vastus Medialis, Vastus Intermedius, Vastus Lateralis
GMAX	Superior, Middle and Inferior Gluteus Maximus
GMED	Anterior, Middle and Posterior Gluteus Medius and Minimus
HAM	Semimembranosus, Semitendinosus, Biceps Femoris Long Head, Gracilis
BFSH	Biceps Femoris Short Head
GAS	Medial Gastrocnemius, Lateral Gastrocnemius
SOL	Soleus, Tibialis Posterior, Flexor Digitorum Longus
TA	Tibialis Anterior, Extensor Digitorum Longus

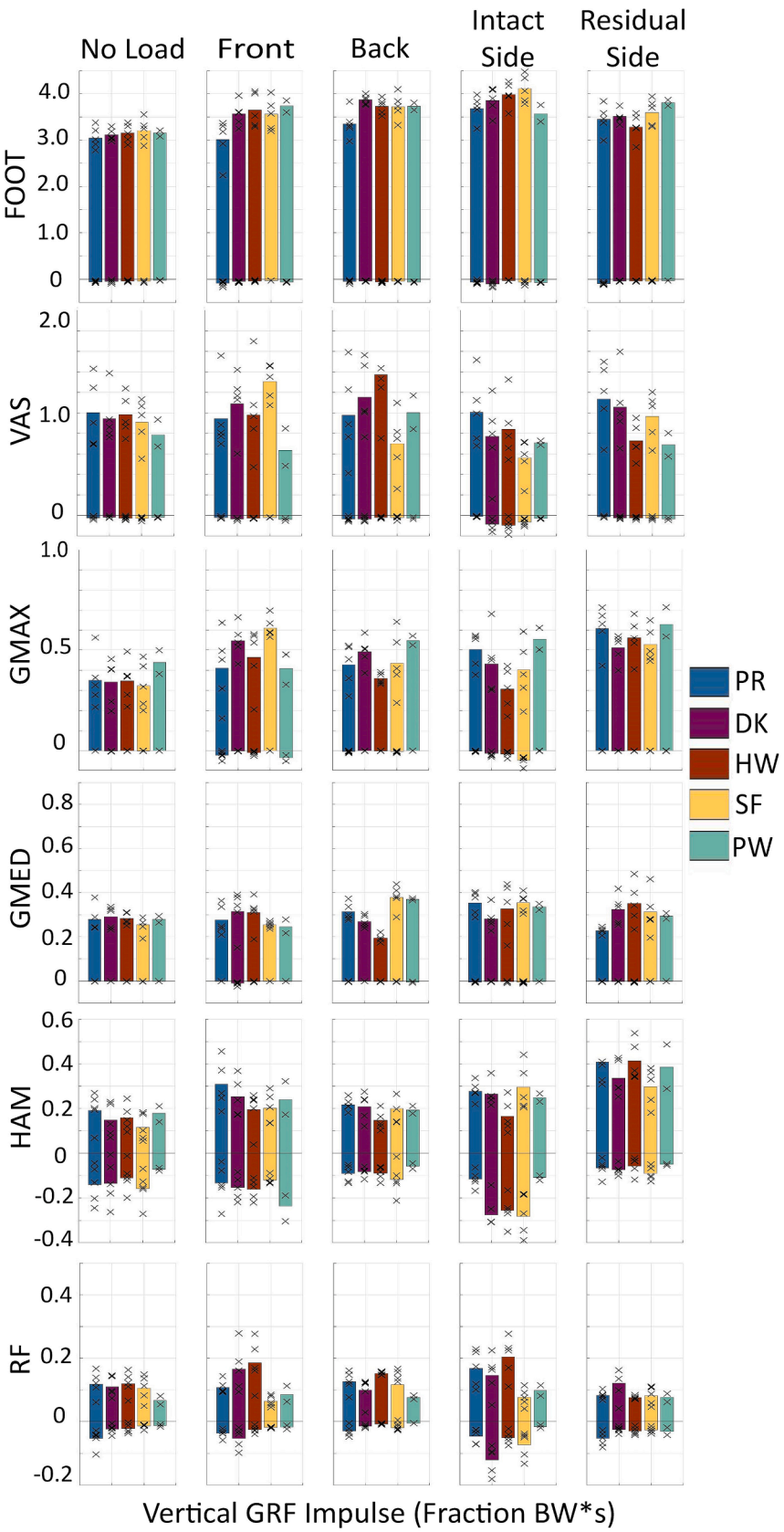

Fig. 1. Average individual muscle contributions of the *residual limb* to body support (vertical ground reaction force) integrated over stance, where individual values are represented with an 'x,' for five different loading conditions (no load, front, back, intact-side and residual-side-loads). Prostheses evaluated include prescribed (PR), dual-keel (DK), prescribed with heel-wedge (HW), one category stiffer (SF) and a powered foot (PW).

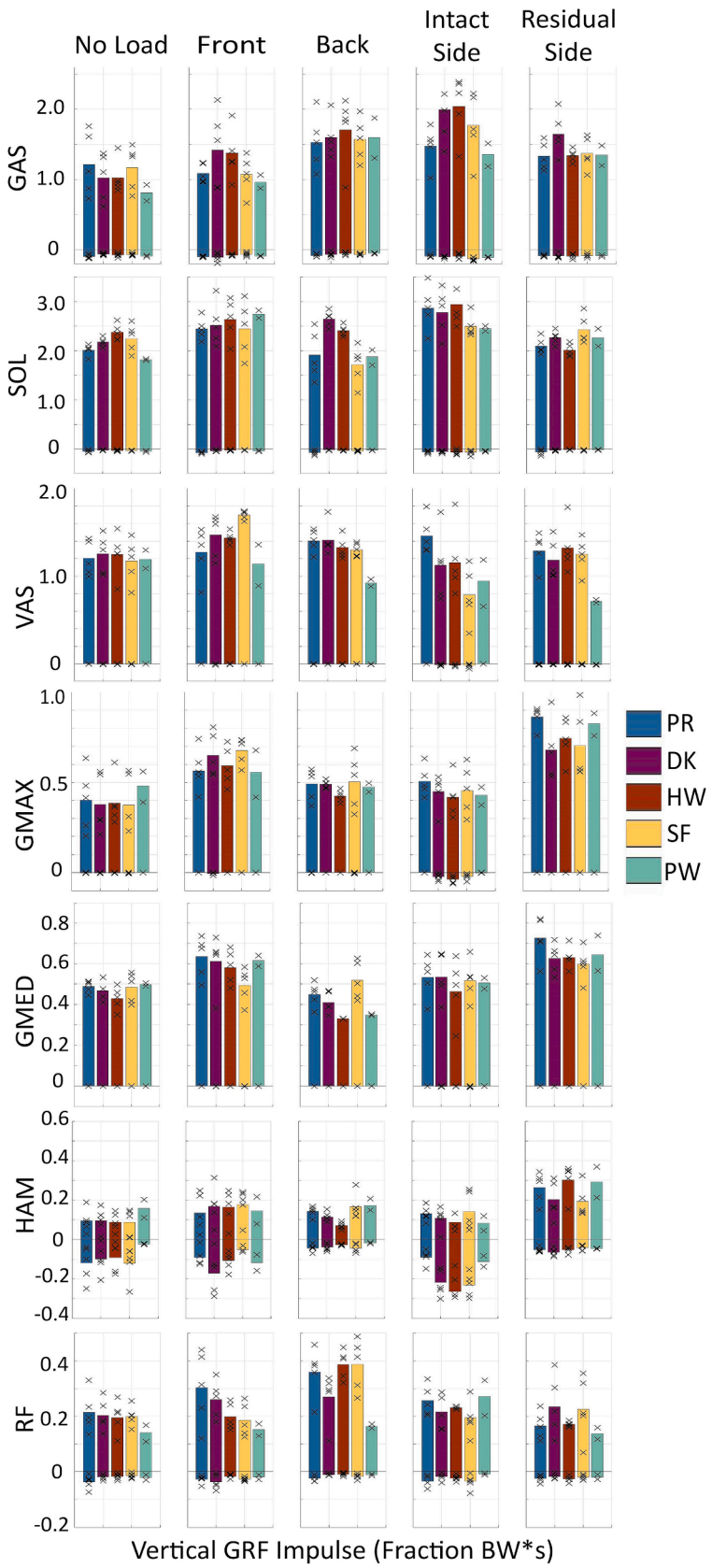

Fig. 2. Average individual muscle contributions of the *intact limb* to body support (vertical ground reaction force) integrated over stance, where individual values are represented with an 'x,' for five different loading conditions (no load, front, back, intact-side and residual-side-loads). Prostheses evaluated include prescribed (PR), dual-keel (DK), prescribed with heel-wedge (HW), one category stiffer (SF) and a powered foot (PW).

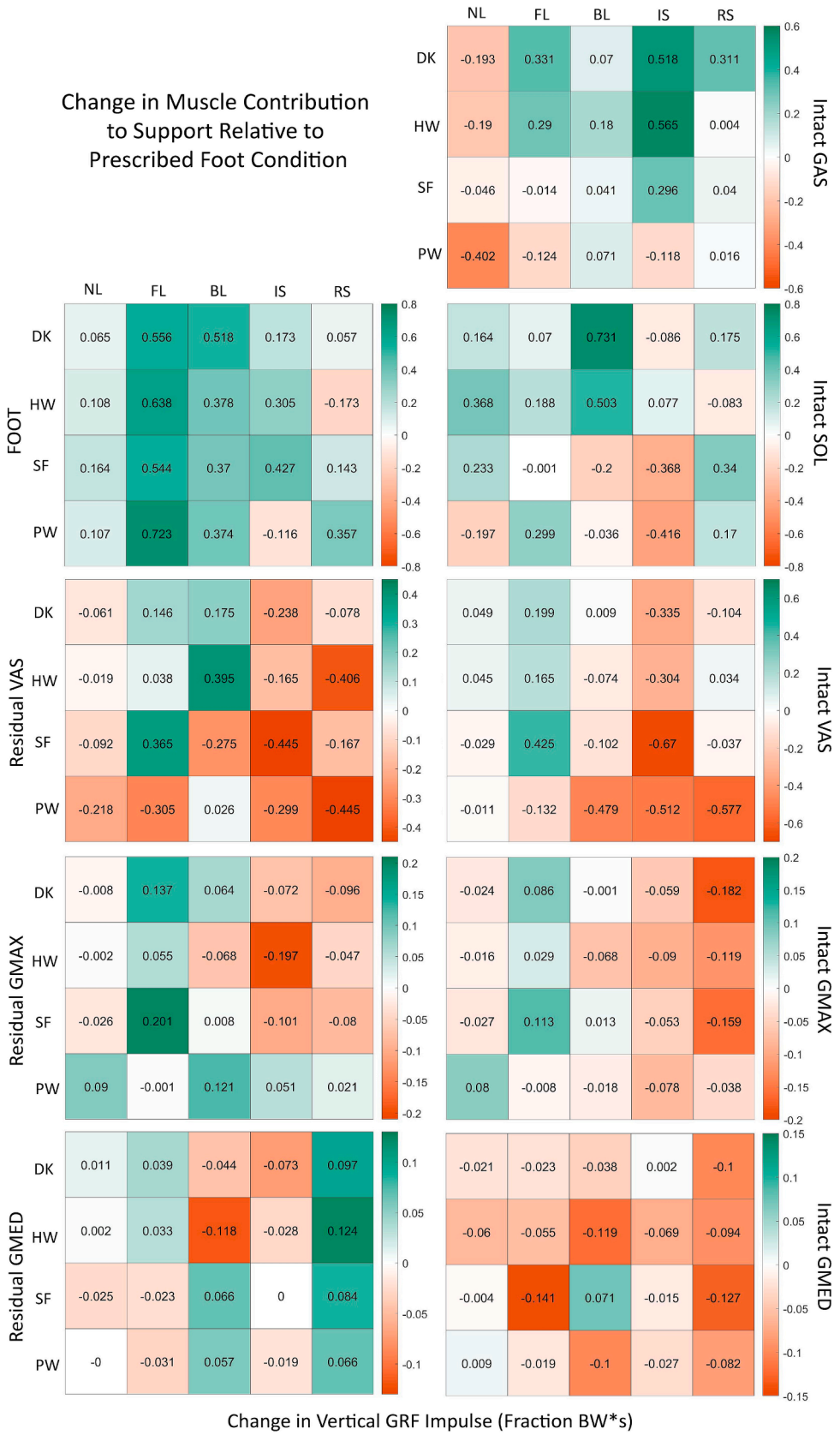

Fig. 3. Average change in contributions to body support (vertical ground reaction force) for four different prostheses (dual-keel (DK), prescribed with heel-wedge (HW), one category stiffer (SF) and a powered foot (PW)) relative to the prescribed (PR) foot condition for the prosthetic Foot, residual VAS, residual GMAX, residual GMED, intact GAS, intact SOL, intact GMAX and intact GMED. Load types evaluated include no load (NL), front (FL), back (BL), intact-side (IS) and residual-side-loads (RS).

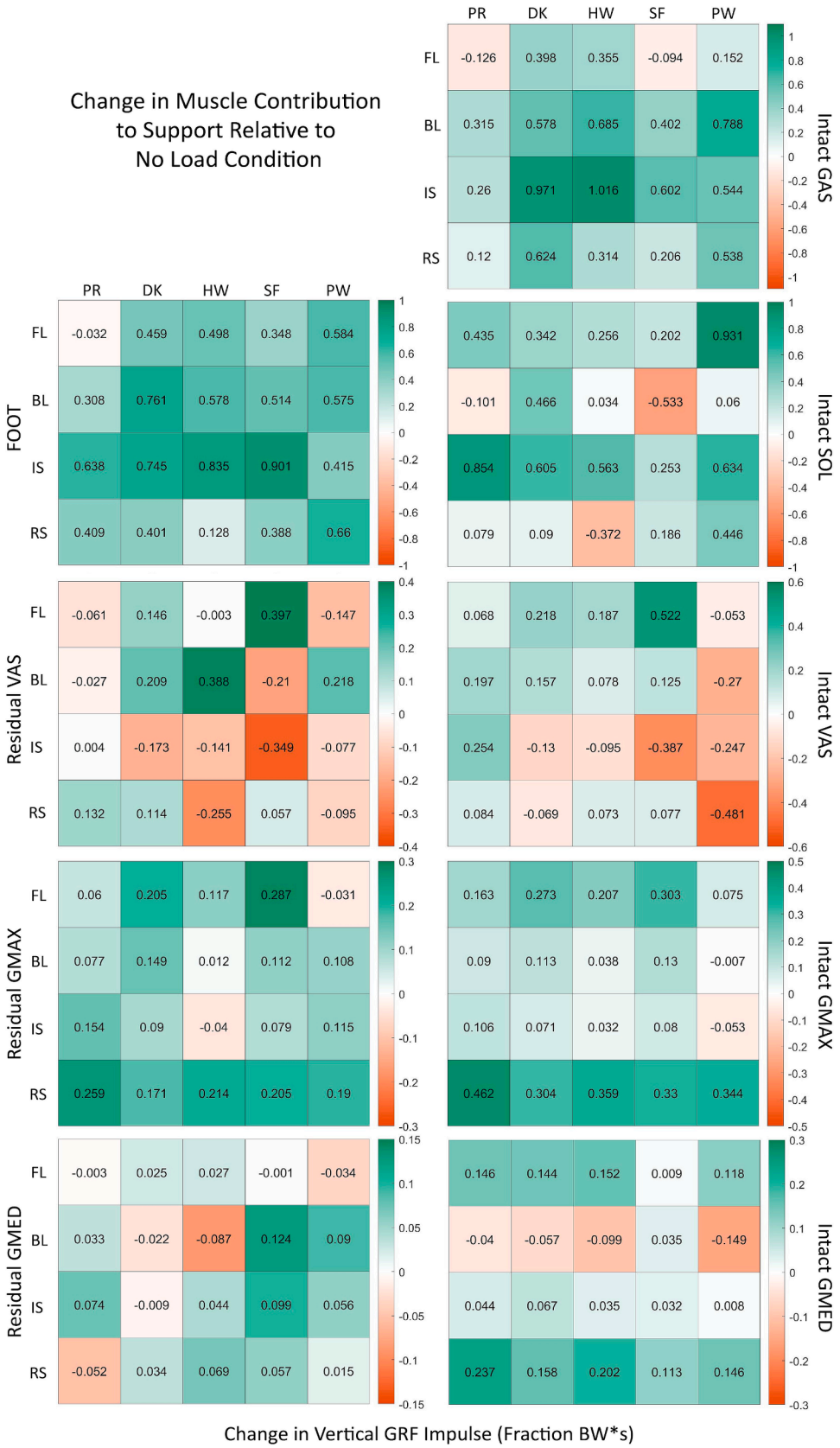

Fig. 4. Average change in contributions to body support (vertical ground reaction force) for four different loading conditions (front (FL), back (BL), intact-side (IS) and residual-side-loads (RS)) relative to no load condition for the prosthetic Foot, residual VAS, residual GMAX, residual GMED, intact GAS, intact SOL, intact GMAX and intact GMED. Prostheses evaluated include prescribed (PR), dual-keel (DK), prescribed with heel-wedge (HW), one category stiffer (SF) and a powered foot (PW).

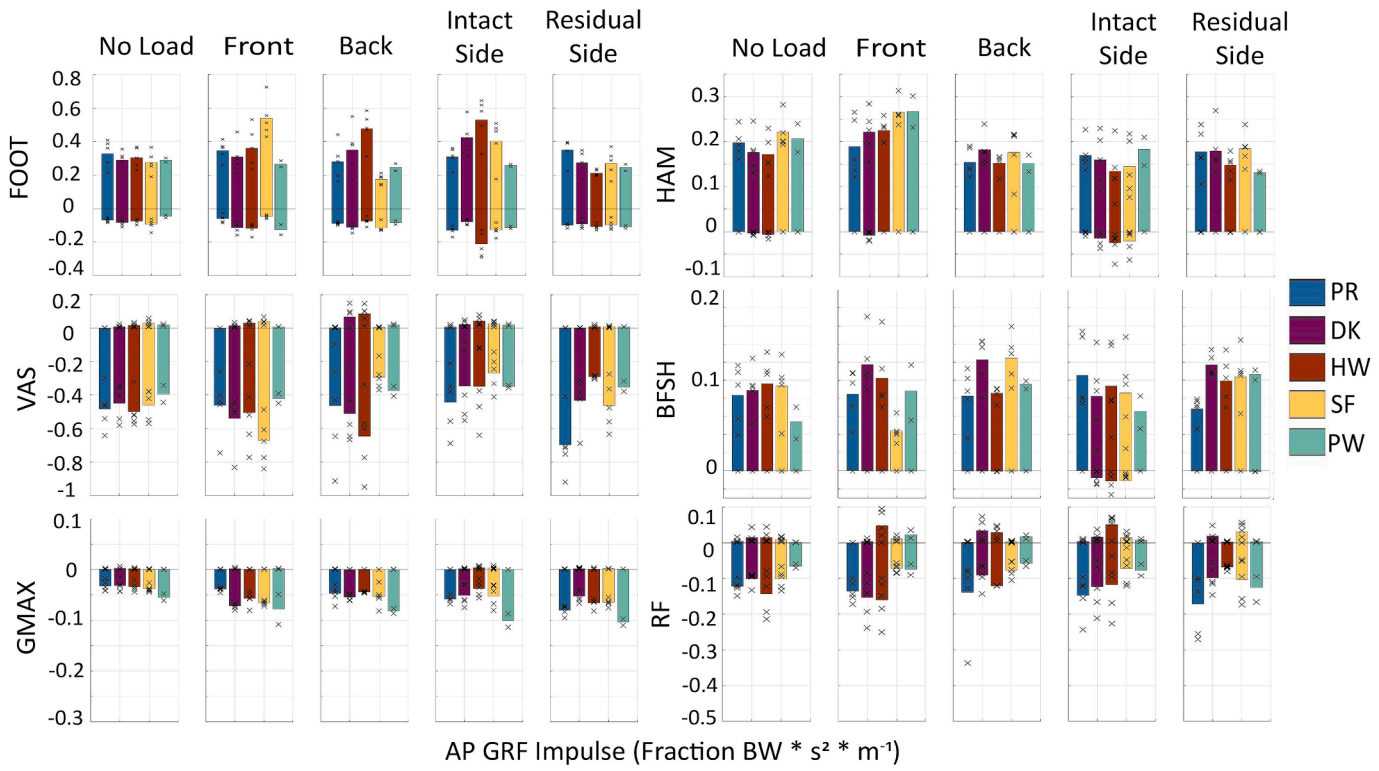

Fig. 5. Average individual muscle contributions of the residual limb to propulsion (anterior-posterior ground reaction force) integrated over stance, where individual values are represented with an 'x,' for five different loading conditions (no load, front, back, intact-side and residual-side-loads). Prostheses evaluated include prescribed (PR), dual-keel (DK), prescribed with heel-wedge (HW), one category stiffer (SF) and a powered foot (PW).

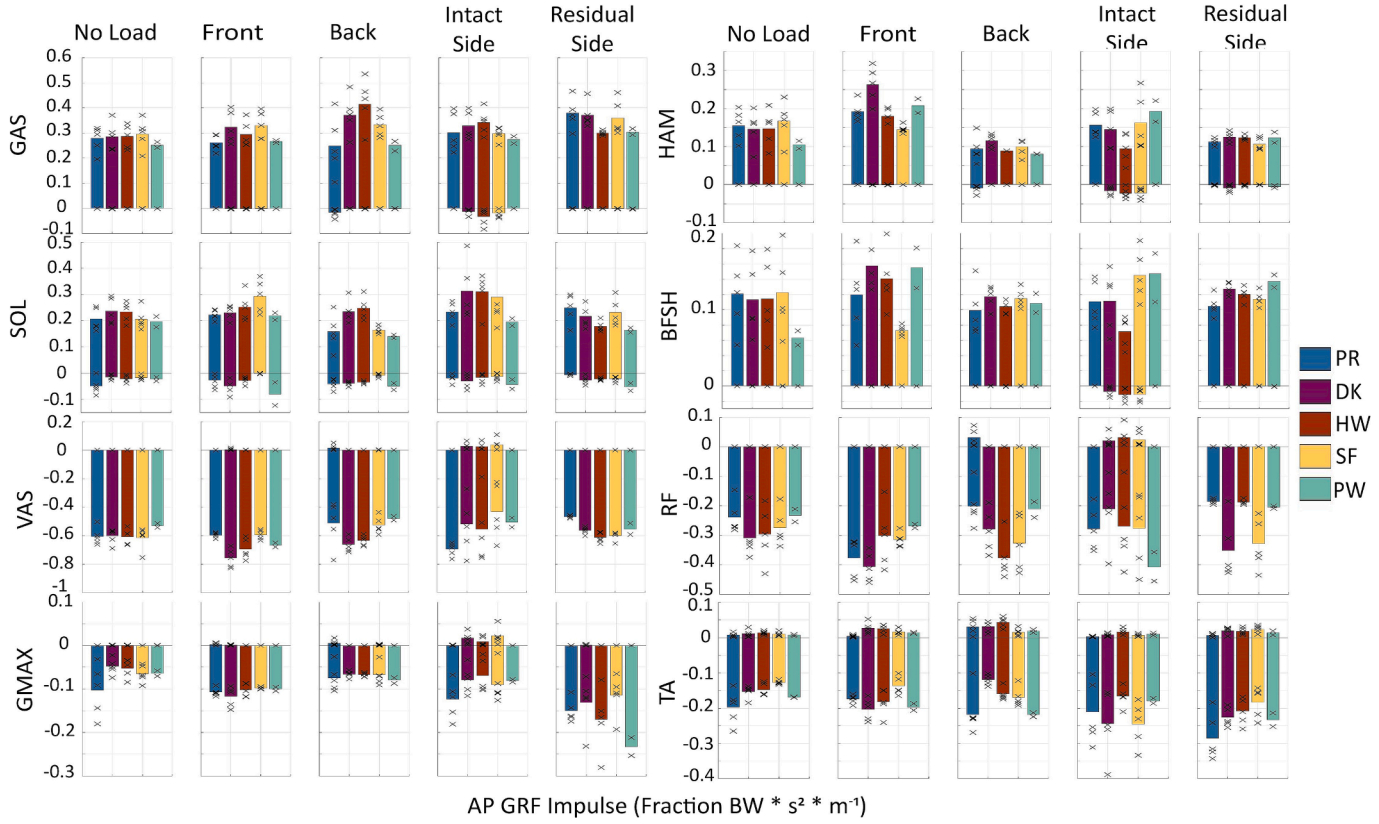

Fig. 6. Average individual muscle contributions of the intact limb to propulsion (anterior-posterior ground reaction force) integrated over stance, where individual values are represented with an 'x,' for five different loading conditions (no load, front, back, intact-side and residual-side-loads). Prostheses evaluated include prescribed (PR), dual-keel (DK), prescribed with heel-wedge (HW), one category stiffer (SF) and a powered foot (PW).

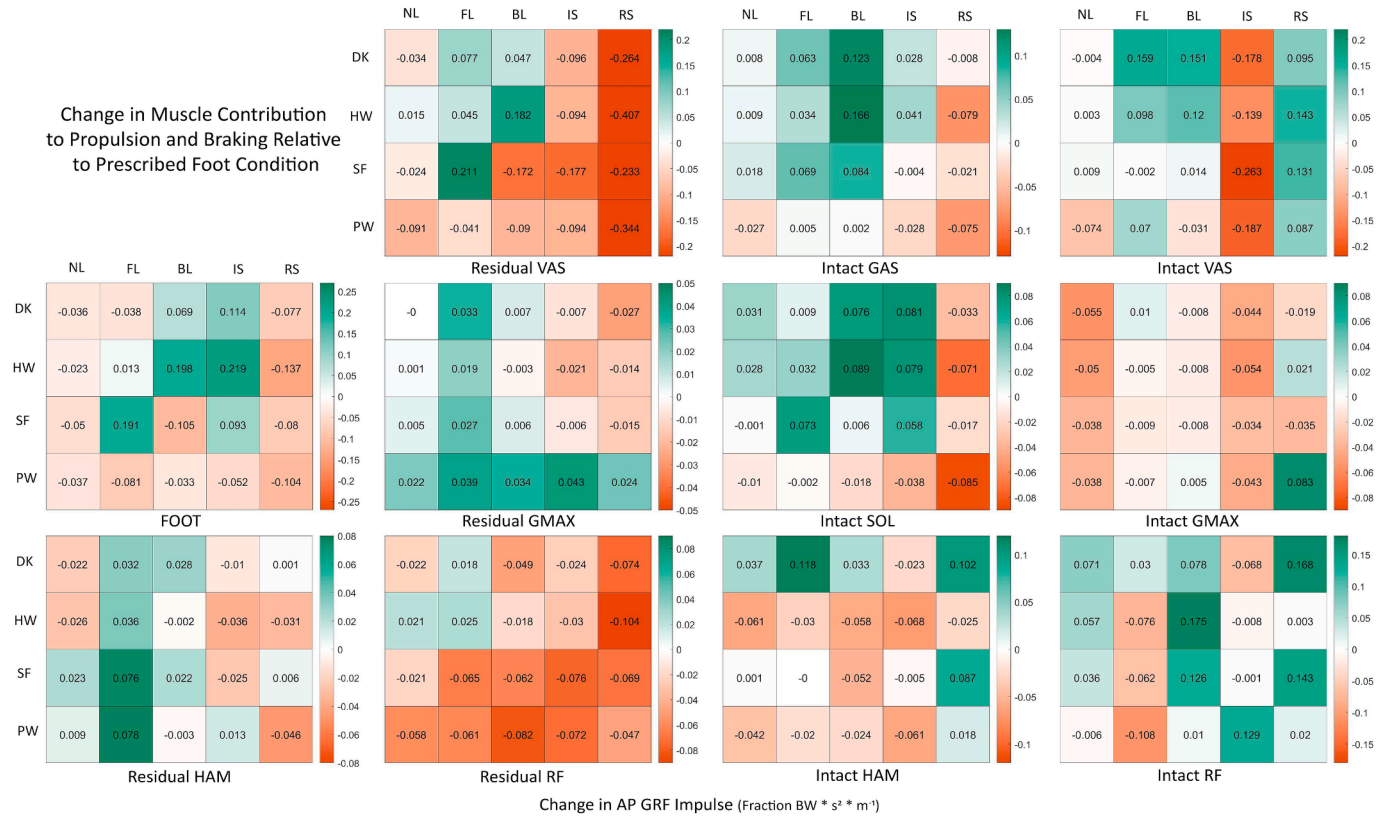

Fig. 7. Average change in contributions to forward propulsion (positive anterior-posterior ground reaction force) for the Foot, residual Ham, intact GAS, intact SOL and intact HAM and braking (negative anterior-posterior ground reaction force) from the residual VAS, residual GMAX, residual RF, intact VAS, intact GMAX and intact RF resulting from dual-keel (DK), prescribed with heel-wedge (HW), one category stiffer (SF) and a powered foot (PW), relative to prescribed (PR) foot. Load types evaluated include no load (NL), front (FL), back (BL), intact-side (IS) and residual-side-loads (RS).

PW foot also generally resulted in reduced plantarflexor contribution to propulsion relative to the PR foot (Fig. 7). Wearing a non-prescribed foot also caused a reduction in HAM_i contribution to propulsion across most prostheses and loading conditions (Fig. 7).

The effect of prosthetic foot on contributions to braking varied substantially between the intact and residual foot. The residual VAS and RF typically displayed reduced contributions to braking for most loading conditions when a non-prescribed foot was worn (Fig. 7). Conversely, when a non-prescribed foot was worn, VAS_i displayed increased contributions to braking, except for the intact-side-loading condition (Fig. 7). The PW foot resulted in increased $GMAX_r$ contribution to braking for all loading conditions, as did the non-prescribed feet for the front-load condition (Fig. 7). However, wearing a non-prescribed foot typically caused a reduced contribution from $GMAX_i$ (Fig. 7).

3.2.2. *Changes relative to the no-load condition*

Loading consistently increased most muscle contributions to support (Fig. 4), but not propulsion (Fig. 8). The muscle contributions to braking from $GMAX_{i,r}$, as well as contributions to propulsion from GAS, all increased in response to load (Fig. 8). The prosthetic foot contribution to forward propulsion typically increased for the front-load while decreasing for the residual-side-load (Fig. 8). The PW foot resulted in reduced prosthetic foot contribution to propulsion during loading relative to the no-load condition (Fig. 8). Conversely, the DK and HW feet resulted in increased contributions for most loading conditions (Fig. 8). The back-, intact-side- and residual-side-loads resulted in lower $HAM_{i,r}$ contributions to forward propulsion, while the front-load resulted in increased contributions (Fig. 8).

4. Discussion

The purpose of this study was to use modeling and simulation to investigate the effects of various prosthetic feet and load conditions on individual muscle and prosthesis contributions to body support and propulsion. We expected that during load carriage, the stiffer prostheses (SF, HW, DK) would result in increased prosthesis contributions to support and propulsion relative to the PR foot, while reducing muscle contributions. While the stiffer feet generally resulted in larger foot contributions to support, this did not translate to reduced muscle contributions. Further, we expected the PW foot would result in the largest foot contributions to support and propulsion for all load conditions. Conversely, we found that the PW foot was not advantageous for most loading conditions as it did not contribute to increased support or propulsion.

Aligned with previous studies, the primary contributors to body support were the prosthetic foot and both the residual and intact GAS, SOL, VAS, GMAX and GMED (Liu et al., 2008; Neptune et al., 2001; Silverman & Neptune, 2012), while the primary contributors to propulsion were the prosthetic foot and plantarflexors and the primary contributors to braking were VAS and RF (Liu et al., 2008; Neptune et al., 2001; Sasaki & Neptune, 2006; Silverman & Neptune, 2012). The prosthetic foot and plantarflexors also contributed to braking during early stance. Relative to the PR foot, all non-prescribed feet resulted in increased foot contributions to support that generally resulted in reduced muscle contributions, except for the front-load condition and plantarflexors. Conversely, they did not consistently result in increased foot contributions to propulsion. This suggests that during load carriage, increasing foot stiffness aids in providing body support, but does not aid in propulsion. Due to their limited deflection, the HW, SF, and DK may result in reduced energy storage and return, while suggesting a trade-off

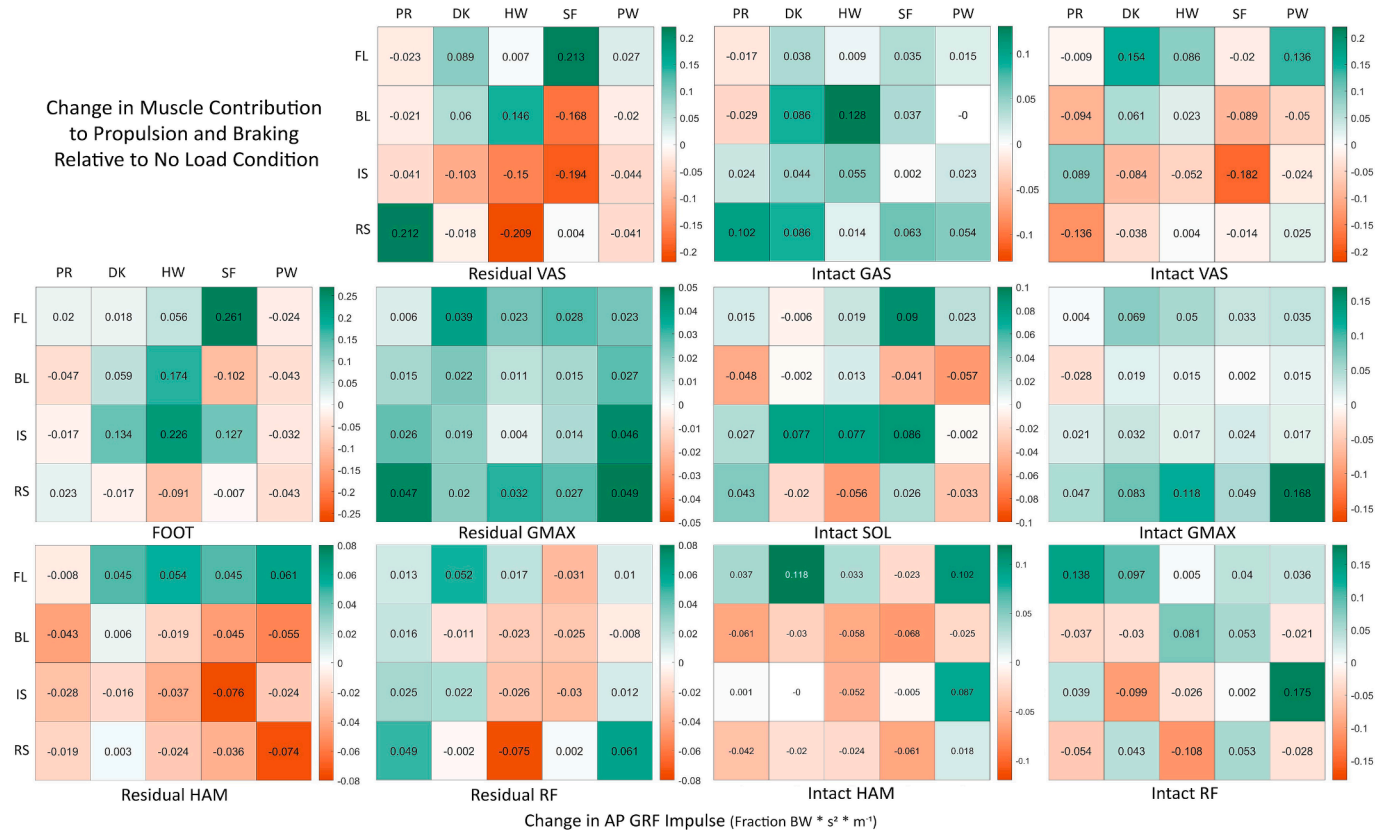

Fig. 8. Average change in contributions to forward propulsion (positive anterior-posterior ground reaction force) for the Foot, residual HAM, intact GAS, intact SOL and intact HAM and braking (negative anterior-posterior ground reaction force) from the residual VAS, residual GMAX, residual RF, intact VAS, intact GMAX and intact RF resulting from front (FL), back (BL), intact-side (IS) and residual-side (RS) loads relative to the no-load (NL) condition. Prostheses evaluated include prescribed (PR), dual-keel (DK), prescribed with heel-wedge (HW), one category stiffer (SF) and a powered foot (PW).

between contributions to support and propulsion, which aligns well with the findings of previous studies (Fey et al., 2011). Unlike previous studies which reported increased trailing residual limb mechanical work (Montgomery & Grabowski, 2018), the PW foot did not improve forward propulsion for the two participants.

4.1. *Effects on muscle contributions to body support*

Most muscles responded to load by increasing their contributions to support. Previous studies found that RF, GMAX, GMED and VAS are primary contributors to body support in early stance during increased load conditions (McGowan et al., 2010; Silder et al., 2013). In contrast, both VAS displayed mixed responses to load carriage depending on the load placement, including during the back-load condition, which had increased contributions for DK and HW feet (aligned with previous studies), but reduced contributions for PR, SF and PW feet (McGowan et al., 2010; Silder et al., 2013). Consistent with others, RF displayed increased contributions to support during load carriage, except for the residual-side-load condition (McGowan et al., 2010; Silder et al., 2013). GMAX displayed notable increases in contribution to support during load carriage. Previous studies found that intact and residual hip extensor moments during early stance are much greater in individuals with TTA than in unimpaired populations, which are believed to compensate for the lack of ankle plantarflexors (e.g., Grumillier et al., 2008; Winter & Sienko, 1988). These results suggest that individuals with TTA respond to the increased demand from load changes by modulating their GMAX and RF, rather than VAS as seen in unimpaired populations.

$GMED_i$ displayed a reduced contribution to support for the back-load condition while generally showing an increased contribution for the other loading conditions. The contribution of $GMED_i$ increased most during the residual-side-load condition. Conversely, the contribution of $GMED_r$ increased most during the intact-side-load condition. These results are consistent with previous studies that indicate that a contralateral load requires increased hip abductor activity, due to an increase internal torque demand (Neumann et al., 1992; Neumann & Hase, 1994), and that GMED is a key contributor in regulating frontal plane whole-body angular momentum and acts to rotate the body towards the ipsilateral leg (Neptune & McGowan, 2016).

Modeling and simulation studies have identified the plantarflexors as being largely responsible for producing the second GRF peak and accelerating the COM during the second half of stance (Liu et al., 2006; McGowan et al., 2010; Neptune et al., 2001), and they are important modulators of body support during load carriage (McGowan et al., 2010; Silder et al., 2013), which is consistent with our findings of increased plantarflexor contributions to support for all loading conditions relative to the no-load condition. Both GAS and the prosthetic foot increased contributions to support for the back-load condition relative to the front-load conditions. This was likely a compensatory mechanism to increase forward angular momentum in the back-load condition during late stance (Neptune & McGowan, 2011).

4.2. *Condition effects on muscle contributions to propulsion*

During load carriage, the plantarflexor contributions to forward propulsion increased more than that of the prosthetic foot (Fig. 8), suggesting increased dependence on their intact limb to generate propulsion relative to no-load. Further, when wearing stiffer feet, the propulsion from the plantarflexors increased notably. The combined increase from the plantarflexors was greater than that of the prosthetic

foot for the back- and front-load condition, also indicating increased dependence on their intact plantarflexors to generate propulsion.

HAM_i contributions to propulsion decreased with the stiffer prosthetic feet (i.e., SF and HW conditions), which aligns with previous work (Fey et al., 2011), while the opposite trend occurred with HAM_r. HAM_i behavior may be a compensatory mechanism to counteract the increased propulsion generated by the plantarflexors when wearing stiffer feet. Similarly, the HAM_r response may be an attempt to increase residual-limb propulsion due to the reduced prosthetic foot contribution to propulsion. Further, $HAM_{i,r}$ contributions to forward propulsion increased during the front-load relative to the no-load condition, while decreasing during the back-load condition. $HAM_{i,r}$ responses were likely a mechanism to increase backwards angular momentum during the front-load condition while reducing backwards angular momentum during the back-load condition (Neptune & McGowan, 2011).

5. Summary

We expected to find an optimal loading position which minimized muscle contributions to body support and propulsion. The results suggest that the ideal loading position depends on the prosthetic foot prescription. Broadly, the front-load condition may be more challenging because it demands increased muscle contributions to support and propulsion across the different prosthetic feet. However, for individuals with plantarflexor weakness, the front- and residual-side-loads may be advantageous since they require less contributions from the plantarflexors to forward propulsion and body support relative to other load carriage conditions. Further, large variability of some muscle contributions (e.g., RF) was observed across all conditions, suggesting that individuals with TTA may rely on a variety of compensatory mechanisms to overcome plantarflexor loss under different load conditions. Further, these results suggest the need for patient-specific prescription as there was a large range of responses to each prosthesis.

6. Limitations

Due to challenges from the COVID-19 pandemic and the extensive nature of the experimental protocol, recruiting participants who were physically capable of safely completing the protocol proved to be challenging, resulting in below-target recruitment numbers. Further research with additional participants is recommended to generalize these findings.

Further, due to the build height of the PW foot, most participants did not have enough pylon length to use the PW foot and data were only collected from two participants. While the PW foot was not advantageous for these participants, powered feet have shown promising results during unloaded gait (e.g., Herr & Grabowski, 2012; Montgomery & Grabowski, 2018). Thus, further research is needed to fully understand whether a powered foot is advantageous under various load carriage conditions.

A potential model limitation is the prosthetic socket and residual limb interface was assumed to be rigid. However, all muscle contributions were identified during the stance phase of gait; thus, negligible socket movement and kinematic error were observed.

All subjects indicated they were comfortable with the foot and load conditions with the provided acclimation period. A longer acclimation period might reduce variability and influence the results, but an IRB-imposed maximum of four hours per study visit limited the time available.

GRF data were collected using five overground force plates, limiting the number of gait cycles collected from each trial. While there were challenges isolating individual foot strikes on instrumented treadmills due to crossover steps, data collected from overground force plates provided easily identifiable GRFs for each foot. However, due to the length of the experimental protocol, we were unable to collect more than one trial of each experimental condition.

CRediT authorship contribution statement

Aude S. Lefranc: Writing – original draft, Visualization, Validation, Methodology, Investigation, Formal analysis, Data curation, Conceptualization. **Glenn K. Klute:** Writing – review & editing, Resources, Project administration, Methodology, Investigation, Funding acquisition, Data curation, Conceptualization. **Richard R. Neptune:** Writing – review & editing, Supervision, Project administration, Methodology, Investigation, Funding acquisition, Conceptualization.

Declaration of competing interest

The authors declare that they have no known competing financial interests or personal relationships that could have appeared to influence the work reported in this paper.

Acknowledgements

This research was supported in part by awards I01 RX003138 and IK6 RX002974 from the United States Department of Veterans Affairs Rehabilitation Research and Development Service.

Appendix A. Supplementary data

Supplementary data to this article can be found online at https://doi.org/10.1016/j.jbiomech.2024.112379.

References

Burke, M.J., Roman, V., Wright, V., 1978. Bone and joint changes in lower limb amputees. Ann. Rheum. Dis. 37 (3), 252–254. https://doi.org/10.1136/ard.37.3.252.

Crosbie, J., Flynn, W., Rutter, L., 1994. Effect of side load carriage on the kinematics of gait. Gait Posture 2 (2), 103–108. https://doi.org/10.1016/0966-6362(94)90099-x.

Delp, S.L., Anderson, F.C., Arnold, A.S., Loan, P., Habib, A., John, C.T., Guendelman, E., Thelen, D.G., 2007. OpenSim: open-source software to create and analyze dynamic simulations of movement. IEEE Trans. Biomed. Eng. 54 (11), 1940–1950. https://doi.org/10.1109/TBME.2007.901024.

Dembia, C.L., Silder, A., Uchida, T.K., Hicks, J.L., Delp, S.L., 2017. Simulating ideal assistive devices to reduce the metabolic cost of walking with heavy loads. PLoS One 12 (7), e0180320.

Doyle, S.S., Lemaire, E.D., Besemann, M., Dudek, N.L., 2014. Changes to level ground transtibial amputee gait with a weighted backpack. Clin. Biomech. 29 (2), 149–154. https://doi.org/10.1016/j.clinbiomech.2013.11.019.

Doyle, S.S., Lemaire, E.D., Besemann, M., Dudek, N.L., 2015. Changes to transtibial amputee gait with a weighted backpack on multiple surfaces. Clin. Biomech. 30 (10), 1119–1124. https://doi.org/10.1016/j.clinbiomech.2015.08.015.

Fey, N.P., Klute, G.K., Neptune, R.R., 2011. The influence of energy storage and return foot stiffness on walking mechanics and muscle activity in below-knee amputees. Clin. Biomech. (Bristol, Avon) 26 (10), 1025–1032. https://doi.org/10.1016/j.clinbiomech.2011.06.007.

Fey, N.P., Klute, G.K., Neptune, R.R., 2012. Optimization of prosthetic foot stiffness to reduce metabolic cost and intact knee loading during below-knee amputee walking: a theoretical study. J. Biomech. Eng. 134 (11). https://doi.org/10.1115/1.4007824.

Grumillier, C., Martinet, N., Paysant, J., André, J.-M., Beyaert, C., 2008. Compensatory mechanism involving the hip joint of the intact limb during gait in unilateral transtibial amputees. J. Biomech. 41 (14), 2926–2931. https://doi.org/10.1016/j.jbiomech.2008.07.018.

Hamner, S.R., Seth, A., Delp, S.L., 2010. Muscle contributions to propulsion and support during running. J. Biomech. 43 (14), 2709–2716. https://doi.org/10.1016/j.jbiomech.2010.06.025.

Herr, H.M., Grabowski, A.M., 2012. Bionic ankle–foot prosthesis normalizes walking gait for persons with leg amputation. Proc. R. Soc. B Biol. Sci. 279 (1728), 457–464. https://doi.org/10.1098/rspb.2011.1194.

Hicks, J.L., Uchida, T.K., Seth, A., Rajagopal, A., Delp, S.L., 2015. Is my model good enough? Best practices for verification and validation of musculoskeletal models and simulations of movement. J. Biomech. Eng. 137 (2), 020905. https://doi.org/10.1115/1.4029304.

LaPrè, A.K., Price, M.A., Wedge, R.D., Umberger, B.R., Sup, F.C., 2018. Approach for gait analysis in persons with limb loss including residuum and prosthesis socket dynamics. Int. J. Numer. Methods in Biomed. Eng. 34 (4), e2936.

Liu, M.Q., Anderson, F.C., Pandy, M.G., Delp, S.L., 2006. Muscles that support the body also modulate forward progression during walking. J. Biomech. 39 (14), 2623–2630. https://doi.org/10.1016/j.jbiomech.2005.08.017.

Liu, M.Q., Anderson, F.C., Schwartz, M.H., Delp, S.L., 2008. Muscle contributions to support and progression over a range of walking speeds. J. Biomech. 41 (15), 3243–3252. https://doi.org/10.1016/j.jbiomech.2008.07.031.

McGowan, C.P., Neptune, R.R., Kram, R., 2008. Independent effects of weight and mass on plantar flexor activity during walking: implications for their contributions to body support and forward propulsion. J. Appl. Physiol. 105 (2), 486–494. https://doi.org/10.1152/japplphysiol.90448.2008.

McGowan, C.P., Kram, R., Neptune, R.R., 2009. Modulation of leg muscle function in response to altered demand for body support and forward propulsion during walking. J. Biomech. 42 (7), 850–856. https://doi.org/10.1016/j.jbiomech.2009.01.025.

McGowan, C.P., Neptune, R.R., Clark, D.J., Kautz, S.A., 2010. Modular control of human walking: Adaptations to altered mechanical demands. J. Biomech. 43 (3), 412–419. https://doi.org/10.1016/j.jbiomech.2009.10.009.

Montgomery, J.R., Grabowski, A.M., 2018. Use of a powered ankle–foot prosthesis reduces the metabolic cost of uphill walking and improves leg work symmetry in people with transtibial amputations. J. R. Soc. Interface 15 (145), 20180442. https://doi.org/10.1098/rsif.2018.0442.

Neptune, R.R., Kautz, S.A., Zajac, F.E., 2001. Contributions of the individual ankle plantar flexors to support, forward progression and swing initiation during walking. J. Biomech. 34 (11), 1387–1398. https://doi.org/10.1016/s0021-9290(01)00105-1.

Neptune, R.R., McGowan, C.P., 2011. Muscle contributions to whole-body sagittal plane angular momentum during walking. J. Biomech. 44 (1), 6–12. https://doi.org/10.1016/j.jbiomech.2010.08.015.

Neptune, R.R., McGowan, C.P., 2016. Muscle contributions to frontal plane angular momentum during walking. J. Biomech. 49 (13), 2975–2981. https://doi.org/10.1016/j.jbiomech.2016.07.016.

Neptune, R.R., Zajac, F.E., Kautz, S.A., 2004. Muscle force redistributes segmental power for body progression during walking. Gait Posture 19 (2), 194–205. https://doi.org/10.1016/S0966-6362(03)00062-6.

Neumann, D.A., Cook, T.M., Sholty, R.L., Sobush, D.C., 1992. An electromyographic analysis of hip abductor muscle activity when subjects are carrying loads in one or both hands. Phys. Ther. 72 (3), 207–217. https://doi.org/10.1093/ptj/72.3.207.

Neumann, D.A., Hase, A.D., 1994. An electromyographic analysis of the hip abductors during load carriage: implications for hip joint protection. J. Orthop. Sports Phys. Ther. 19 (5), 296–304. https://doi.org/10.2519/jospt.1994.19.5.296.

Pandy, M.G., Lin, Y.-C., Kim, H.J., 2010. Muscle coordination of mediolateral balance in normal walking. J. Biomech. 43 (11), 2055–2064. https://doi.org/10.1016/j.jbiomech.2010.04.010.

Robinson, J.L., Smidt, G.L., Arora, J.S., 1977. Accelerographic, temporal, and distance gait: factors in below-knee amputees. Phys. Ther. 57 (8), 898–904. https://doi.org/10.1093/ptj/57.8.898.

Sanderson, D.J., Martin, P.E., 1997. Lower extremity kinematic and kinetic adaptations in unilateral below-knee amputees during walking. Gait Posture 6 (2), 126–136. https://doi.org/10.1016/S0966-6362(97)01112-0.

Sasaki, K., Neptune, R.R., 2006. Differences in muscle function during walking and running at the same speed. J. Biomech. 39 (11), 2005–2013. https://doi.org/10.1016/j.jbiomech.2005.06.019.

Schnall, B.L., Wolf, E.J., Bell, J.C., Gambel, J., Bensel, C.K., 2012. Metabolic analysis of male servicemembers with transtibial amputations carrying military loads. J. Rehabil. Res. Dev. 49 (4), 535–544. https://doi.org/10.1682/jrrd.2011.04.0075.

Schnall, B.L., Hendershot, B.D., Bell, J.C., MSE, & Wolf, E. J., 2014. Kinematic analysis of males with transtibial amputation carrying military loads. J. Rehabil. Res. Dev. 51 (10), 1505–1514. https://doi.org/10.1682/JRRD.2014.01.0022.

Seth, A., Hicks, J.L., Uchida, T.K., Habib, A., Dembia, C.L., Dunne, J.J., Ong, C.F., DeMers, M.S., Rajagopal, A., Millard, M., Hamner, S.R., Arnold, E.M., Yong, J.R., Lakshmikanth, S.K., Sherman, M.A., Ku, J.P., Delp, S.L., 2018. OpenSim: Simulating musculoskeletal dynamics and neuromuscular control to study human and animal movement. PLoS Comput. Biol. 14 (7), e1006223.

Silder, A., Delp, S.L., Besier, T., 2013. Men and women adopt similar walking mechanics and muscle activation patterns during load carriage. J. Biomech. 46 (14), 2522–2528. https://doi.org/10.1016/j.jbiomech.2013.06.020.

Silverman, A.K., Neptune, R.R., 2012. Muscle and prosthesis contributions to amputee walking mechanics: A modeling study. J. Biomech. 45 (13), 2271–2278. https://doi.org/10.1016/j.jbiomech.2012.06.008.

Simpkins, C., Ahn, J., Yang, F., 2022. Effects of anterior load carriage on gait parameters: A systematic review with meta-analysis. Appl. Ergon. 98, 103587. https://doi.org/10.1016/j.apergo.2021.103587.

Singh, T., Koh, M., 2009. Effects of backpack load position on spatiotemporal parameters and trunk forward lean. Gait Posture 29 (1), 49–53. https://doi.org/10.1016/j.gaitpost.2008.06.006.

Walsh, G.S., Low, D.C., 2021. Effects of backpack load position on spatiotemporal parameters and trunk forward lean. Appl. Ergon. 93, 103376. https://doi.org/10.1016/j.apergo.2021.103376.

Winter, D.A., Sienko, S.E., 1988. Biomechanics of below-knee amputee gait. J. Biomech. 21 (5), 361–367. https://doi.org/10.1016/0021-9290(88)90142-X.

Zajac, F.E., Neptune, R.R., Kautz, S.A., 2003. Biomechanics and muscle coordination of human walking. Gait Posture 17 (1), 1–17. https://doi.org/10.1016/S0966-6362(02)00069-3.

Zmitrewicz, R.J., Neptune, R.R., Sasaki, K., 2007. Mechanical energetic contributions from individual muscles and elastic prosthetic feet during symmetric unilateral transtibial amputee walking: A theoretical study. J. Biomech. 40 (8), 1824–1831. https://doi.org/10.1016/j.jbiomech.2006.07.009.